PAPER

Comparing two non-equilibrium approaches to modelling of a free-burning arc

To cite this article: M Baeva *et al* 2013 *Plasma Sources Sci. Technol.* **22** 065017

Plasma Sources Sci. Technol. **22** (2013) 065017 (9pp) doi:10.1088/0963-0252/22/6/065017

Comparing two non-equilibrium approaches to modelling of a free-burning arc

M Baeva[1], D Uhrlandt[1], M S Benilov[2] and M D Cunha[2]

[1] Leibniz Institute for Plasma Science and Technology, Felix-Hausdorff-Strasse 2, 17489 Greifswald, Germany
[2] Departamento de Física, CCCEE, Universidade da Madeira, Largo do Município, 9000 Funchal, Portugal

E-mail: baeva@inp-greifswald.de and benilov@uma.pt

Received 19 July 2013, in final form 18 October 2013
Published 29 November 2013
Online at stacks.iop.org/PSST/22/065017

Abstract
Two models of high-pressure arc discharges are compared with each other and with experimental data for an atmospheric-pressure free-burning arc in argon for arc currents of 20–200 A. The models account for space-charge effects and thermal and ionization non-equilibrium in somewhat different ways. One model considers space-charge effects, thermal and ionization non-equilibrium in the near-cathode region and thermal non-equilibrium in the bulk plasma. The other model considers thermal and ionization non-equilibrium in the entire arc plasma and space-charge effects in the near-cathode region. Both models are capable of predicting the arc voltage in fair agreement with experimental data. Differences are observed in the arc attachment to the cathode, which do not strongly affect the near-cathode voltage drop and the total arc voltage for arc currents exceeding 75 A. For lower arc currents the difference is significant but the arc column structure is quite similar and the predicted bulk plasma characteristics are relatively close to each other.

(Some figures may appear in colour only in the online journal)

1. Introduction

Arc discharges are used in a wide range of applications (e.g. gas-tungsten welding, dc plasma torches and high-intensity discharge (HID) lamps, to mention a few). Modelling of arc discharges involves a description of the complex interplay between the electromagnetic field, fluid flow and heat transfer and represents a challenging task. The number of works on this topic is extremely high; see [1, 2] and references therein. However, a universally accepted approach is still absent. In fact, arc models used in different simulation works are highly diverse.

In some models (e.g. [3–7]), the electrodes are not included in the simulations; instead, given distributions of the temperature and electric current density are assumed on the cathode surface and a given distribution of the temperature is assumed on the anode surface. Obviously, relying on assumed distributions makes such a modelling approach somewhat empirical, therefore the electrodes are included in the computational domain in many models.

Lots of models use the assumption of local thermodynamic equilibrium, or LTE, in the whole plasma volume. Some models account for discrepancies between the temperatures of electrons and heavy particles (thermal non-equilibrium) in the whole plasma volume while retaining the assumption of ionization equilibrium; see [4, 5]. Some models account for deviations from ionization equilibrium in the whole plasma volume but retain the assumption of thermal equilibrium; see [8–12]. There are also models that account for deviations from both thermal and ionization equilibrium in the whole plasma volume; see [13–16]. Many models pay special attention to deviations from LTE occurring in near-electrode plasma layers; see [17] and references therein. However, different models of the non-equilibrium near-electrode plasma layers are employed by different authors. Some models assume the near-cathode voltage drop to be very small (less than 1 or

2 V) and neglect space-charge effects in the cathode boundary layer, while others predict near-cathode voltages of about 10 V or higher and consider the effect of the cathode space-charge sheath as crucial; see the discussion in [19].

Thus, models of arc discharges employed by different authors are not only highly diverse, but are based on different, and in some cases even contradictory, physical grounds. Amazingly, there has been little comparison between different models and the question of which effects have to be taken into account for the model to be physically justified remains open.

A step in the latter direction was taken in [19], where electrical characteristics of a free-burning atmospheric-pressure argon arc calculated by means of two models are given. One model accounts for deviations from thermal, but not ionization, equilibrium in the bulk plasma and for space-charge effects and deviations from thermal and ionization equilibrium occurring in the near-cathode region. In the following, this model will be referred to as the 2T-sheath model. The other is the LTE model. Arc voltages given by the two models are compared with each other and with the experiment [25]. It is shown that the 2T-sheath model predicts the arc voltage, which exhibits a variation with the arc current (I) similar to that revealed by the experiment and exceeds experimental values by no more than approximately 2 V in the range $I = 20$–175 A. The sheath contributes about two-thirds or more of the arc voltage. The LTE model overestimates both the resistance of the bulk of the arc column and the resistance of the part of the column that is adjacent to the cathode, and this overestimation to a certain extent compensates, in the current range $I \gtrsim 120$ A, for the neglect of the sheath voltage. As a consequence, the LTE model predicts a course of the arc voltage with the arc current different from the experiment and appreciably underestimates the experimental values for $I \sim 100$ A or lower, although by no more than approximately 2 V for $I \gtrsim 120$ A.

Thus, a physically justified arc discharge model must adequately describe the near-cathode space-charge sheath, i.e. must take into account space-charge effects and deviations from thermal and ionization equilibrium occurring in the near-cathode region. Furthermore, a physically justified arc discharge model must take into account thermal non-equilibrium in the bulk plasma, which is necessary for an adequate description of transport of electric power deposited into the near-cathode sheath to the bulk plasma by electron current [19, 20]. These two requirements restrict the range of existing models of arc discharges that may be considered as physically justified. However, they do not define a unique model: models may take into account, or not, the ionization non-equilibrium in the bulk plasma; besides, models may differ in descriptions of the non-equilibrium near-cathode layer and coupling of the near-cathode layer with the bulk plasma. With the aim to shed light on the effect of these differences, two models are compared in this work with each other and with the experiment. One is the 2T-sheath model [18, 19]. The other is the model of [21], which takes into account deviations from thermal and ionization equilibrium in the bulk plasma and employs models of the near-cathode layer and its coupling with the bulk plasma different from those employed in the 2T-sheath model.

The outline of the papers is as follows. A summary of the main features of the 2T-sheath model and the nonLTE-sheath model with an emphasis on similarities and differences between the models is given in section 2. Results given by the models for conditions of experiments with a 1 cm-long free-burning arc in atmospheric-pressure Ar [25] are presented in section 3. Concluding remarks are summarized in section 4.

2. Main features of the models

The 2T-sheath model and the nonLTE-sheath model are described in detail in [18, 19] and in [21], respectively; here only a brief summary is given outlining their similarities and differences.

In both the 2T-sheath and nonLTE-sheath models, the bulk plasma is assumed to be quasi-neutral with unequal electron and heavy-particle temperatures, $T_e \neq T_h$. The governing differential equations comprise the Navier–Stokes equations, equations of energy for the heavy particles and electrons, the equation of continuity of electric current supplemented with Ohm's law, and Ampère's law for the self-induced magnetic field. The nonLTE-sheath model also comprises a species conservation equation written to take account of diffusion, convection and reactions. In the framework of the 2T-sheath model, ionization equilibrium is assumed to hold in the bulk plasma and the Saha equation is employed.

Note that the bulk plasma model developed in [21] and used in this work as one of the constituents of the nonLTE-sheath model allows for different levels of reaction complexity [22]. For the sake of a reasonable computational cost required for investigation of a wide range of parameters, the model with the simplest reaction scheme and a two-level representation of the atomic argon energy structure is used in this work. The model comprises two heavy species: atoms in the ground state and singly charged ions.

The electrodes in both the 2T-sheath and nonLTE-sheath models are simulated by solving the heat conduction equation in the electrode body. The voltage drop and the effect of Joule heating in the cathode body are small under conditions considered in this work as shown by numerical results [23]. The effect of Joule heating in the anode body is smaller still. Therefore, inclusion in the electrode model of the equation of continuity of electric current supplemented with Ohm's law, which is required for some conditions where the Joule heating plays a role [23], is unnecessary for the conditions considered. Nevertheless, the equation of current continuity can be included for generality and/or technical reasons, and this is done in the case of anode in the 2T-sheath model [18, 19] and in the cases of both cathode and anode in the nonLTE-sheath model [21].

The near-electrode space-charge sheath, while being of central importance for cathodes, plays a minor role for anodes; see the discussion in [17]. Therefore, there is no interface between the bulk plasma and the anode in both the 2T-sheath and nonLTE-sheath models: the electrostatic potential and the normal component of the energy flux density are continuous and temperatures of the heavy particles and the cathode surface coincide. In both models, the normal derivative of the electron temperature vanishes at the anode surface and the density of energy flux to the anode surface is evaluated as the sum of heat fluxes transported by the heavy particles and electrons and of an additional term, which accounts for heating of the anode surface due to condensation of electrons and is proportional to the enthalpy of electron gas.

Both models comprise an interface between the bulk plasma and the cathode. In the case of the 2T-sheath model, the interface accounts for the existence of the near-cathode space-charge sheath and the ionization layer (a region of quasi-neutral plasma adjacent to the sheath where deviations from ionization equilibrium are localized and the ion flux to the cathode is generated) with the assumption of ionization equilibrium at the edge of the ionization layer. In the nonLTE-sheath model, the ionization layer belongs to the bulk plasma and is described by the bulk plasma model; therefore, the interface accounts for only the space-charge sheath. The sheath in both models is assumed to be collisionless for the ions with Boltzmann-distributed plasma electrons and is described along the same lines. The heavy-particle temperature on the bulk plasma side of the interface coincides with the cathode surface temperature. There is a jump of potential in the interface, which represents the near-cathode voltage drop. The normal component of the energy flux density is also discontinuous due to a very substantial electric power deposited by the arc power supply into the near-cathode space-charge sheath. (Note that the concept of a high-pressure arc cathode being heated by the energy flux generated in a thin near-cathode plasma layer, which is sometimes called the model of non-linear surface heating, is well known, validated experimentally and widely used for low-current arcs (e.g. [26]); see [17] and references therein.) Electric current and energy flux to the cathode surface are evaluated by means of expressions that are similar in both models and account for contributions of the ions, plasma electrons and emitted electrons.

The nonLTE-sheath model [21] is realized on the computational platform [24], which does not allow much freedom in the choice of boundary condition for the equation of electron energy in the bulk plasma. In particular, it is not possible to introduce into this boundary condition an account of energy originating in acceleration of the emitted electrons in the space-charge sheath. For this reason, the nonLTE-sheath model [21] involves the equation of balance of the electron energy in the ionization layer, which accounts for this energy. This is the same equation that appears in the 2T-sheath model; however, it is employed in a different way. In the 2T-sheath model, this equation governs the local electron temperature in the near-cathode layer, which then serves as a boundary condition for the equation of electron energy in the bulk plasma. In the nonLTE-sheath model [21], the equation of balance of the electron energy in the ionization layer governs the local value of the near-cathode voltage drop.

In both models, the electrostatic potential at the base of the anode is set equal to zero and the potential of the cathode surface is computed. The computed potential should be constant along the cathode surface to the accuracy of the (small) voltage drop inside the electrodes; however, in reality there are small variations in both models. In the 2T-sheath model [18, 19], this is a price paid for speeding up the computations by means of avoiding iterations between the code describing the cathode and the near-cathode layer and the code describing the arc column and the anode, which is achieved by neglecting variations of the near-cathode voltage drop from one point of the arc attachment to the other. (These variations are typically below 1 V, as shown by simulations [18].) In the nonLTE-sheath model [21], this is a price paid for the possibility of using the platform [24], which is achieved by means of computing the near-cathode voltage drop as described in the preceding paragraph. For definiteness, we indicate that the terms 'arc column voltage' and 'arc voltage' as used in the following refer to the voltage drop in the bulk plasma and the inter-electrode voltage (i.e. arc column voltage plus the near-cathode voltage drop) evaluated along the arc axis.

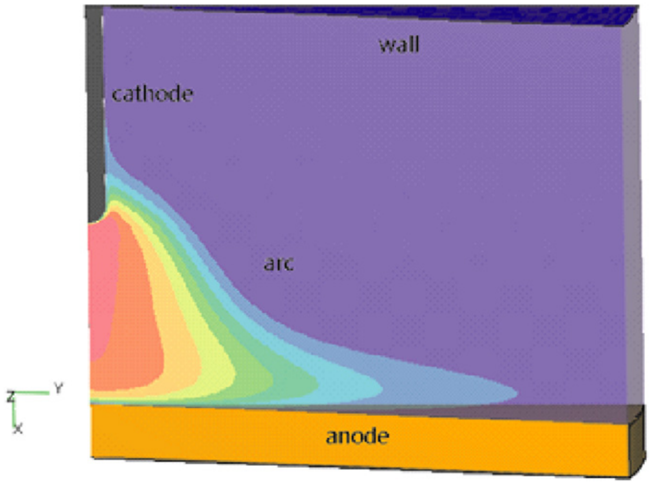

Figure 1. The computational domain.

3. Results and discussion

The simulations performed by means of the 2T-sheath model for the experimental conditions and arrangement [25] are reported in [18]. In this work, simulations for the same conditions have been performed by means of the nonLTE-sheath model. A comparison between the results is given in this section.

A sketch of the computational domain is shown in figure 1. The cathode is a cylindrical tungsten rod with a radius of 1 mm and a hemispherical tip. The anode is flat and made of copper. The base of the cathode is considered with a temperature equal to the ambient temperature of 300 K. The anode is cooled and its outer part is also considered to have a temperature of 300 K. The distance between the cathode and the anode is 10 mm. The arc chamber is closed. The arc current in the experiments [25] varied over the range 20–175 A.

3.1. Electrical characteristics

Figure 2 presents the calculated arc column voltage, the near-cathode voltage drop and the total of both (the total arc voltage) obtained by means of the 2T-sheath model and the nonLTE-sheath model. Experimental values of the arc voltage [25] are shown using solid symbols for a diffuse arc attachment and

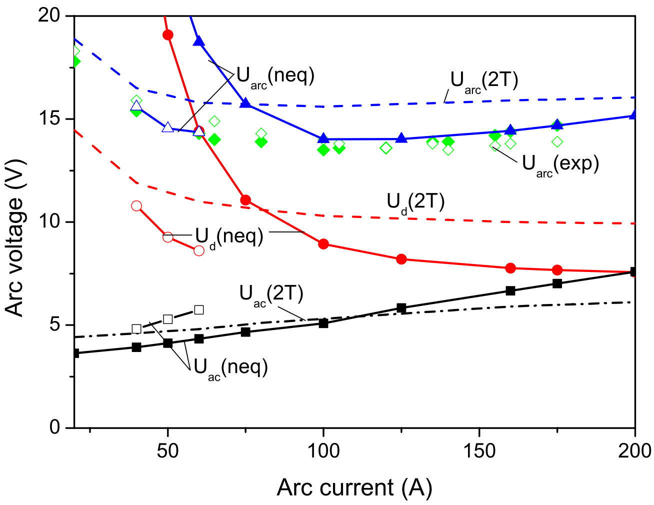

Figure 2. Total arc voltage U_{arc} obtained: experimentally (exp), from the 2T-sheath model (2T), and from the nonLTE-sheath model (neq). Near-cathode voltage drop U_d obtained with the 2T-sheath model (2T) and the nonLTE-sheath model (neq). Arc column voltage U_{ac} obtained with the 2T-sheath model (2T) and the nonLTE-sheath model (neq).

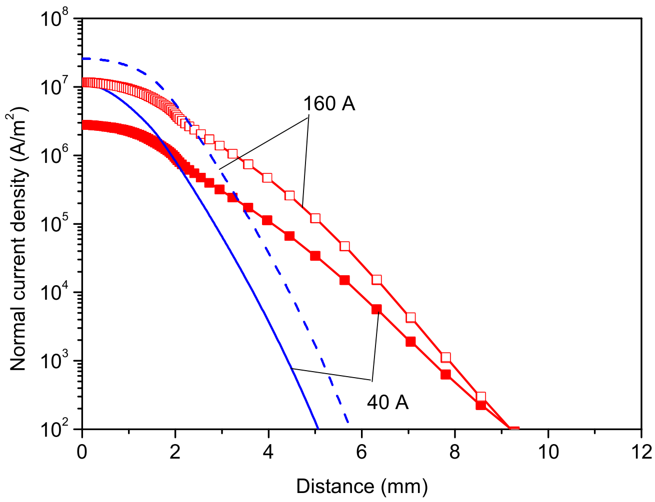

Figure 3. Distributions of the density of electric current from the plasma along the cathode surface computed by means of the 2T-sheath model (lines) and the nonLTE-sheath model (lines with symbols).

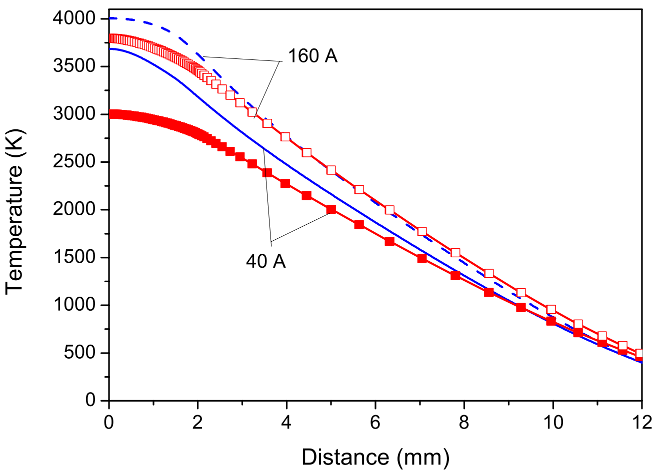

Figure 4. Distributions of temperature along the cathode surface from the 2T-sheath model (lines) and the nonLTE-sheath model (lines with symbols).

open symbols for a contracted arc attachment. The values of both regimes do not differ significantly. The results of the 2T-sheath model (dashed lines) show an increase in the arc column voltage and a decrease in the near-cathode voltage drop with increasing arc current. As a result, the total arc voltage first decreases with increasing arc current and then starts slightly increasing. These results are in fair agreement with the experiment: they follow the same course and the numerical difference does not exceed 1–2 V in the current range 20–175 A. The arc column voltage predicted by the nonLTE-sheath model is rather close to that predicted by the 2T-sheath model. The difference in values of the near-cathode voltage drop is more significant, especially at lower currents. The total arc voltage predicted by the nonLTE-sheath model for arc currents between 100 and 200 A is somewhat lower than that predicted by the 2T-sheath model and shows very good agreement with the experimental values. At lower arc currents, the calculated arc voltage increases faster than that predicted by the 2T-sheath model and the experimental values, which is due to the higher values of the near-cathode voltage drop.

The difference in the values of the near-cathode voltage drop may be understood as follows. The normal component of the density of electric current from the plasma to the cathode is shown in figure 3 as a function of the distance measured along the generatrix from the centre of the front surface of the cathode. The current density predicted by the 2T-sheath model on the arc axis is higher than the corresponding value from the nonLTE-sheath model by a factor of about 4 for arc current of 40 A and by a factor of 2.2 for 160 A. In other words, the 2T-sheath model predicts a more constricted arc attachment than the nonLTE-sheath model. The smaller size of the arc attachment area results further in higher temperatures of the cathode tip (figure 4) in case of the 2T-sheath model. These differences do not strongly affect the near-cathode voltage drop for currents exceeding approximately 75 A; however, for lower currents they result in the 2T-sheath model predicting a significantly lower near-cathode voltage drop and consequently lower arc voltage values, which fit the experimental values.

As described in section 2, the difference between descriptions of plasma–cathode interaction used in the two models is that the ionization layer, i.e. a region of quasi-neutral plasma adjacent to the sheath where the ion flux to the cathode is generated, is treated as a part of the near-cathode layer in the framework of the 2T-sheath model and as a part of the bulk plasma in the nonLTE-sheath model. This difference is consistent with the different descriptions of the bulk plasma employed in the two models (thermal non-equilibrium and ionization equilibrium in the 2T-sheath model and thermal non-equilibrium and ionization non-equilibrium in the nonLTE-sheath model) and is therefore natural and

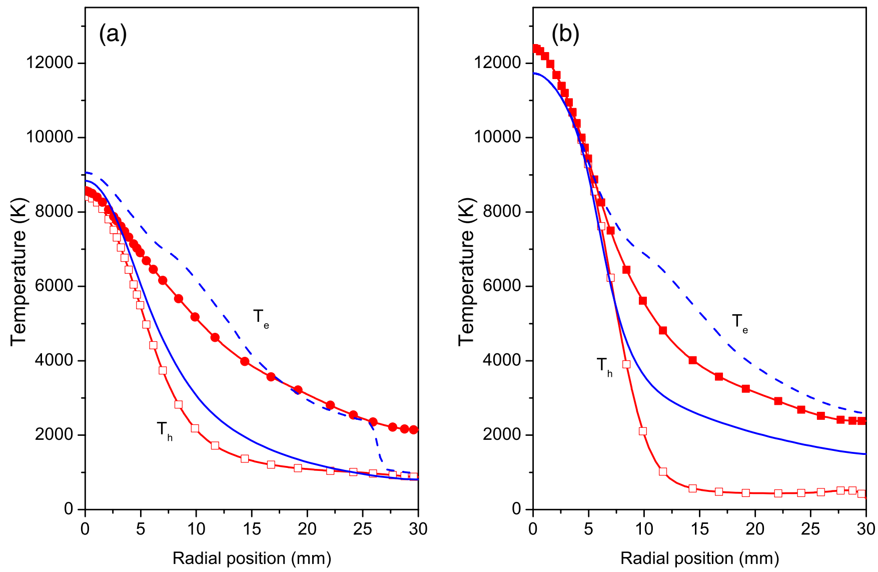

Figure 5. Temperatures of electrons and heavy particles in the midplane of the arc. Results from the 2T-sheath model (lines) and the nonLTE-sheath model (lines with symbols) for arc currents of (*a*) 40 A and (*b*) 160 A.

appropriate. There are also differences in the numerical realization, in particular, in the way of determination of the near-cathode voltage (the method employed in the nonLTE-sheath model was devised in order to enable the use of the simulation platform [24]). The question as to which one of these differences leads to the above-described difference in the arc attachments predicted by the two models remains unanswered for now.

The above-mentioned proximity of the arc column voltages predicted by the nonLTE-sheath and the 2T-sheath models suggests that the arc column voltage is not strongly affected by the size of arc attachment to the cathode. In order to check this suggestion, simulations were performed by means of the nonLTE-sheath model with current collection being (artificially) restricted to a circle of radius equal to 1/2 of the cathode radius. The arc column voltage, the sheath voltage and the arc voltage obtained for $I = 40$ A, 50 A, 60 A are shown in figure 2 by lines with open symbols (rectangles, circles and triangles, respectively). One can see that the arc column voltage indeed has not changed significantly; an important result which is discussed in some detail in the next section. In contrast, the sheath voltage drop and hence the arc voltage are significantly reduced, the latter coming into agreement with the experimental values.

The models being employed do not take into account specific phenomena occurring in the near-anode plasma layer. More accurate models indicate that the anode fall potential is in the range of 1 or 2 V and is negative in most cases, including in the case of diffuse arc attachment ([27–31]; see [32] for further references and discussion). Therefore, it is possible that the computed values of arc voltage shown in figure 2 should be reduced by up to 2 V. Then the data from the 2T-sheath model would become a little closer to the experiment and the data from the nonLTE-sheath model for arc currents between 100 and 200 A will slightly deviate from the experiment; however, the overall pattern would not change.

3.2. Characteristics of the arc column

Figures 5–8 present radial distributions in the midplane of the arc and distributions along the arc axis of the electron and heavy-particle temperatures, the electric conductivity and the axial component of the electric current density. Note that the origin is positioned on the base of the cathode and the cathode height is 12 mm, so the axial position in plots with distributions of plasma parameters along the arc axis varies in the range from 12 up to 22 mm.

One can see from figure 5(*a*) that for the arc current of 40 A the electron temperature in the midplane predicted by the nonLTE-sheath model is slightly lower than that predicted by the 2T-sheath model on the arc axis and in its vicinity; the two distributions virtually coincide for radial positions between 15 and 25 mm. Radial distributions of the heavy-particle temperature are also close. Distributions of electron temperature along the arc axis (figure 6(*a*)) are close as well, although values predicted by the 2T-sheath model are slightly lower than those from the nonLTE-sheath model near the cathode and by about 1000 K higher near the anode. Axial distributions of the heavy-particle temperature almost coincide. For an arc current value of 160 A (figures 5(*b*) and 6(*b*)), the deviations between the two models are somewhat higher (for example, the heavy-particle temperature predicted by the 2T-sheath model in the midplane exceeds that from the nonLTE-sheath model by about 2000 K for radial positions around 15 mm); however, the overall agreement remains good.

Distributions of the electric conductivity in the midplane of the arc (figure 7(*a*)) predicted by the two models differ, but are close once again; values from the 2T-sheath model are by about 10% lower. Differences in the axial distributions (figure 7(*b*)) are more pronounced, especially in the vicinity of the cathode (which is not surprising given the difference in the description of plasma–cathode interaction and the assumption of ionization equilibrium in the bulk plasma used in the

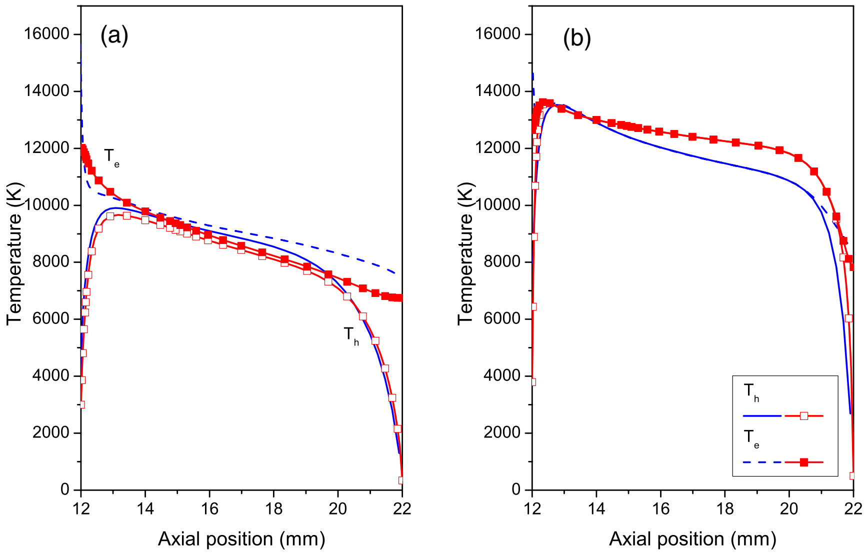

Figure 6. Temperatures of electrons and heavy particles along the arc axis. Results from the 2T-sheath model (lines) and the nonLTE-sheath model (lines with open symbols) for arc currents of (*a*) 40 A and (*b*) 160 A.

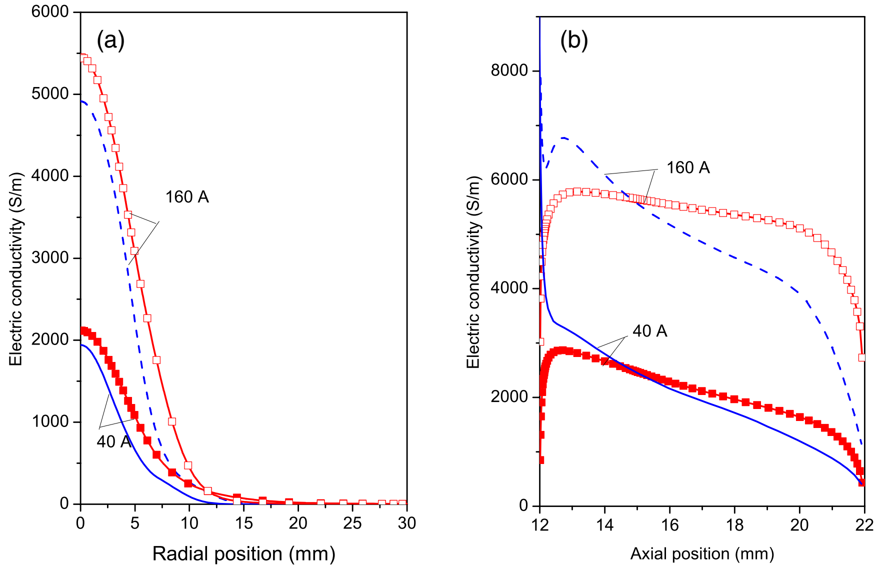

Figure 7. Distributions of the electrical conductivity (*a*) in the midplane of the arc and (*b*) along the arc axis. Results from the 2T-sheath model (lines) and the nonLTE-sheath model (lines with symbols).

2T-sheath model). In the arc body, the difference is larger for an arc current of 160 A, but is still below 30%.

Figure 8 presents the distributions of the axial component of the electric current density. The main difference between the results obtained in the 2T-sheath model and the nonLTE-sheath model concerns the low-current case and the region close to the arc axis where the values predicted in the 2T-sheath model are higher by about 40%. In the high-current case, the values agree within 3% for axial positions up to 17 mm and within 10% for the rest of the arc.

Results of simulations performed by means of the nonLTE-sheath model with current collection being restricted to a circle of radius equal to 1/2 of the cathode radius are shown in figure 9. The arc current density at the cathode surface (figure 9(*a*)) is higher by a factor of approximately 3–4 in the case of restricted arc attachment; however, this difference rapidly decreases as one moves into the plasma and becomes small for axial positions beyond 14 mm. The so-called Maecker effect, i.e. acceleration of the arc plasma in front of the cathode by the Lorentz force, is stronger in the case of restricted arc attachment: the axial components of the flow velocity (figure 9(*b*)) differ in their maximum values by about 40% and in the arc body by about 20%. Distributions of potential (figure 9(*c*)) do not differ substantially; the arc column voltage increases by about 18–25%.

In summary, one can say that the significant differences in the arc attachment to the cathode do not significantly affect the arc column structure and voltage drop. In particular, this means that the Maecker effect does not considerably affect the arc column voltage under the conditions considered.

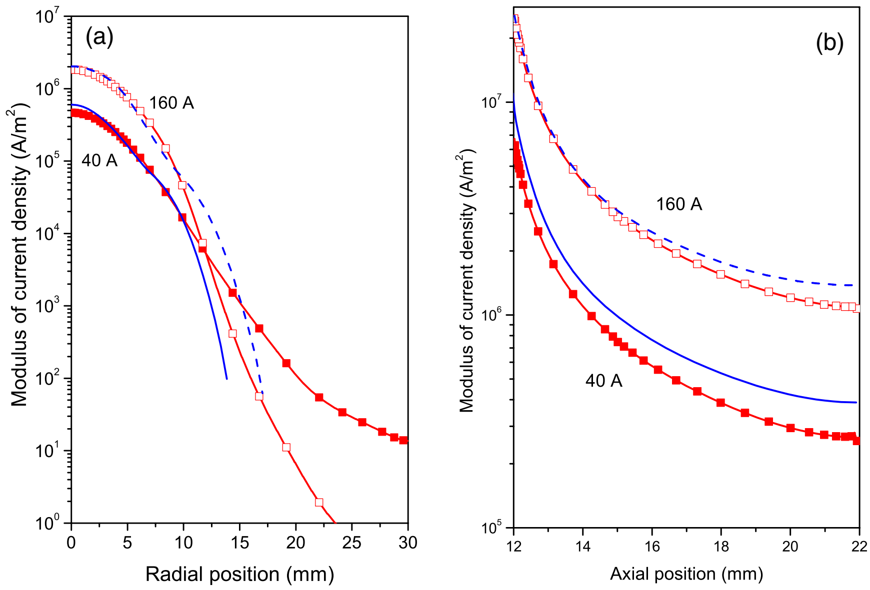

Figure 8. Axial current density (*a*) in the midplane of the arc and (*b*) along the arc axis. Results from the 2T-sheath model (lines) and the nonLTE-sheath model (lines with symbols).

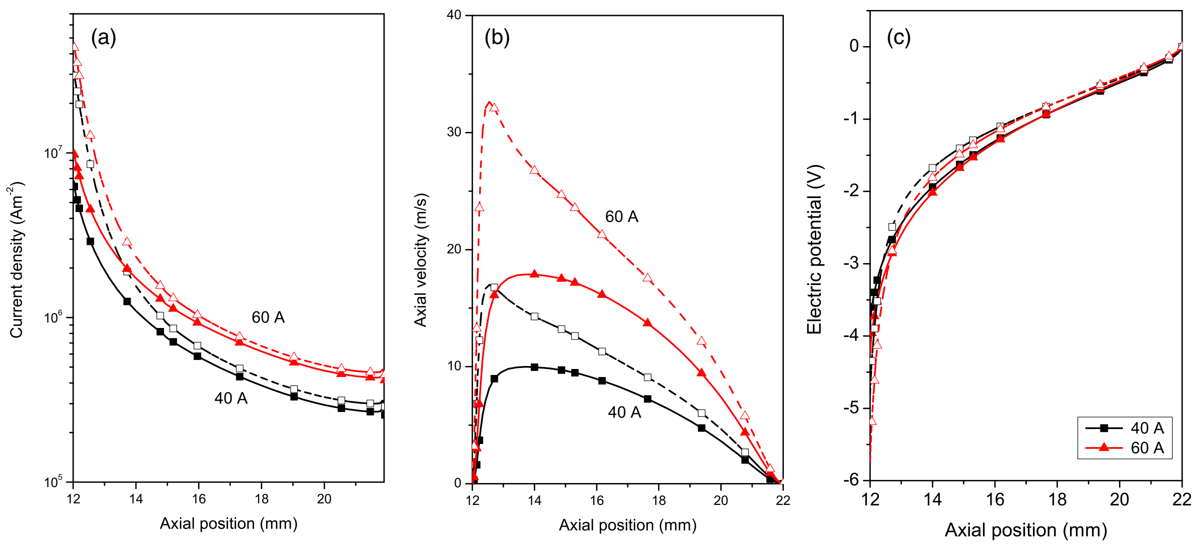

Figure 9. Results of the nonLTE-sheath model with restricted current collection (lines with open symbols) and free current collection (lines with solid symbols).

4. Summary and conclusion

A very substantial electrical power is deposited by the arc power supply into the space-charge sheath near the cathode of a high-pressure arc discharge. A part of this power is transported into the bulk plasma by electron current and the rest goes to the cathode. Therefore, physically justified models of high-pressure arc discharges should take into account space-charge effects and deviations from thermal and ionization equilibrium occurring in the near-cathode region and thermal non-equilibrium in the bulk plasma. In this work, two such models are compared with each other and with the experiment [25], performed on a 1 cm-long free-burning arc in atmospheric-pressure Ar. One of these models, termed the 2T-sheath model, is the model [18, 19] that accounts for thermal non-equilibrium in the whole arc volume and for space-charge effects and deviations from ionization equilibrium occurring in the near-cathode region. The other one, termed the nonLTE-sheath model, is the model [21] that accounts for thermal and ionization non-equilibrium in the whole arc volume and for space-charge effects in the near-cathode region. In addition to the different accounts of ionization non-equilibrium implemented in the models and different sets of kinetic and transport coefficients used, the models differ in assumptions concerning the plasma–cathode interaction made in order to facilitate numerical realization and/or speed up the computations.

The 2T-sheath model predicts a more constricted and, consequently, hotter arc attachment to the cathode than the nonLTE-sheath model. These differences do not strongly affect the near-cathode voltage drop for currents exceeding approximately 75 A; however, for lower currents they result in a significantly lower near-cathode voltage drop predicted by the 2T-sheath model.

The significant differences in the arc attachment to the cathode do not considerably affect the arc column structure: the two models predict distributions of bulk plasma characteristics that are relatively close to each other. Also close are the values of the voltage drop in the arc column. The latter means that the Maecker effect does not significantly affect the arc column voltage under the conditions considered, which is also confirmed by simulations in the framework of the nonLTE-sheath model with artificially limited arc attachment to the cathode.

The two models predict values of arc voltage that are close to each other and experimental values for arc currents between 100 and 200 A. For lower currents the near-cathode voltage drop predicted by the nonLTE-sheath model rapidly increases and the arc voltage predicted by this model is significantly higher than that predicted by the 2T-sheath model and the experimental values. The arc voltage predicted by the 2T-sheath model remains close to the experiment for all currents down to 20 A.

Additional effort is required to improve both models, in particular, relaxing assumptions concerning plasma–cathode interaction made in order to facilitate numerical realization and/or speed up the computations. An extension of the models to treat the near-anode layer at the same level of accuracy as the cathode layer is also scheduled for future work. Considering the complex behaviour of the arc attachment on the cathode under experimental conditions especially at low arc currents (off-axis cathode spots [25]), a three-dimensional modelling could provide a better understanding of the processes.

Acknowledgments

The work at the Leibniz Institute for Plasma Science and Technology was supported by the DFG (German Science Foundation) under grant UH 106/6-1.

The work at Universidade da Madeira was supported by FCT-Fundação para a Ciência e a Tecnologia of Portugal through the projects PTDC/FIS-PLA/2708/2012 Modelling, understanding, and controlling self-organization phenomena in plasma-electrode interaction in gas discharges: from first principles to applications and PEst-OE/MAT/UI0219/2011 Centro de Ciências Matemáticas.

References

[1] Gleizes A, Gonzalez J J and Freton P 2005 Thermal plasma modelling *J. Phys. D: Appl. Phys.* **38** R153

[2] Murphy A B, Tanaka M, Yamamoto K, Tashiro S, Sato T and Lowke J J 2009 Modelling of thermal plasmas for arc welding: the role of the shielding gas properties and of metal vapour *J. Phys. D: Appl. Phys.* **42** 194006

[3] Hsu K C, Etemadi K and Pfender E 1983 Study of the free-burning high-intensity argon arc *J. Appl. Phys.* **54** 1293

[4] Hsu K C and Pfender E 1983 Two-temperature modelling of the free-burning, high-intensity argon arc *J. Appl. Phys.* **54** 4359

[5] Freton P, Gonzalez J J, Ranarijaona Z and Mougenot J 2012 Energy equation formulations for two-temperature modelling of 'thermal' plasmas *J. Phys. D: Appl. Phys.* **45** 465206

[6] Kovitya P and Lowke J J 1985 Two-dimensional analysis of free burning arcs in argon *J. Phys. D: Appl. Phys.* **18** 53

[7] Zhou X and Heberlein J 1995 Characterization of the arc cathode attachment by emission spectroscopy and comparison to theoretical predictions *Plasma Chem. Plasma Process.* **16** S229

[8] Fischer E 1987 Modelling of low-power high-pressure discharge lamps *Philips J. Res.* **42** 58

[9] Flesch P and Neiger M 2005 Understanding anode and cathode behaviour in high-pressure discharge lamps *J. Phys. D: Appl. Phys.* **38** 3098

[10] Lowke J J and Tanaka M 2006 LTE-diffusion approximation for arc calculations *J. Phys. D: Appl. Phys.* **39** 3634

[11] Sansonnens L, Haidar J and Lowke J J 2000 Prediction of properties of free burning arcs including effects of ambipolar diffusion. *J. Phys. D: Appl. Phys.* **33** 148

[12] Tanaka Y, Michishita T and Uesugi Y 2005 Hydrodynamic chemical non-equilibrium model of a pulsed arc discharge in dry air at atmospheric pressure *Plasma Sources Sci. Technol.* **14** 134

[13] Amakawa T, Jenista J, Heberlein J V R and Pfender E 1998 Anode-boundary-layer behaviour in a transferred, high-intensity arc *J. Phys. D: Appl. Phys.* **31** 2826

[14] Haidar J 1999 Non-equilibrium modelling of transferred arcs *J. Phys. D: Appl. Phys.* **32** 263

[15] Gonzalez J J, Girard R and Glezes A 2000 Decay and post-arc phases of a SF_6 arc plasma: a thermal and chemical non-equilibrium model *J. Phys. D: Appl. Phys.* **33** 2759

[16] Baeva M and Uhrlandt D 2011 Non-equilibrium simulation of the spatial and temporal behavior of a magnetically rotating arc in argon *Plasma Sources Sci. Technol.* **20** 035008

[17] Benilov M S 2008 Understanding and modeling plasma–electrode interaction in high-pressure arc discharges: a review *J. Phys. D: Appl. Phys.* **41** 144001

[18] Benilov M S, Benilova L G, Li H-P and Wu G-Q 2012 Sheath and arc-column voltages in high-pressure arc discharges *J. Phys. D: Appl. Phys.* **45** 355201

[19] Li H-P and Benilov M S 2007 Effect of a near-cathode sheath on heat transfer in high-pressure arc plasmas *J. Phys. D: Appl. Phys.* **40** 2010

[20] Almeida N A, Benilov M S and Naidis G V 2008 Unified modelling of near-cathode plasma layers in high-pressure arc discharges *J. Phys. D: Appl. Phys.* **41** 245201

[21] Baeva M, Kozakov R, Gorchakov S and Uhrlandt D 2012 Two-temperature chemically non-equilibrium modelling of transferred arcs *Plasma Sources Sci. Technol.* **21** 055027

[22] Baeva M and Uhrlandt D 2013 Plasma chemistry in the free-burning Ar arc *J. Phys. D: Appl. Phys.* **46** 325202

[23] Benilov M S and Cunha M D 2013 Joule heat generation in thermionic cathodes of high-pressure arc discharges *J. Appl. Phys.* **113** 063301

[24] 2010 CFD-ACE+, ESI CFD Inc., Version 2010

[25] Mitrofanov N K and Shkol'nik S M 2007 Two-forms of attachment of an atmospheric-pressure direct-current arc in argon to a thermionic cathode *Tech. Phys.* **52** 711

[26] Dabringhausen L, Langenscheidt O, Lichtenberg S, Redwitz M and Mentel J 2005 Different modes of arc attachment at HID cathodes: simulation and comparison with measurements *J. Phys. D: Appl. Phys.* **38** 3128

[27] Nemchinskii V A and Perets L N 1977 Near-anode layer of high-current high-pressure arc *Sov. Phys.—Tech. Phys.* **22** 1083

[28] Dinulescu H A and Pfender E 1980 Analysis of the anode boundary layer of high intensity arcs *J. Appl. Phys.* **51** 3149

[29] Nazarenko I P and Panevin I G 1989 Analysis of the near-anode process characters in argon arc discharges of high pressure *Contrib. Plasma Phys.* **29** 251

[30] Jenista J, Heberlein J V R and Pfender E 1997 Numerical model of the anode region of high-current electric arcs *Trans. Plasma Sci.* **25** 883

[31] Yang G and Heberlein J 2007 Anode attachment modes and their formation in a high intensity argon arc. *Plasma Sources Sci. Technol.* **16** 529

[32] Heberlein J, Mentel J and Pfender E 2010 The anode region of electric arcs: a survey *J. Phys. D: Appl. Phys.* **43** 023001